View metadata, citation and similar papers at core.ac.uk
brought to you by CORE
provided by NASA Technical Reports Server

N92-14091

AN EXTENDED KALMAN FILTER FOR SPINNING SPACECRAFT ATTITUDE ESTIMATION

by
David F. Baker
NASA - Goddard Space Flight Center
Attitude Analysis Section (554.1)
Greenbelt, MD 20771

ABSTRACT

An extended Kalman filter for real-time ground attitude estimation of a gyro-less spinning spacecraft has been developed and tested. The filter state vector includes the angular momentum direction, phase angle, inertial nutation angle, and inertial and body nutation rates. The filter solves for the nutating three-axis attitude and accounts for effects due to principle axes offset from the body axes. The attitude is propagated using the kinematics of a rigid body symmetric about the principle spin axis; disturbance torques are assumed to be small. Filter updates consist only of the measured angles between celestial objects (Sun, Earth, etc.) and the nominal spin axis, and the times these angles were measured.

Both simulated data and real data from the Dynamics Explorer -A (DE-A) spacecraft were used to test the filter; the results are presented. Convergence was achieved rapidly from a wide range of a priori state estimates, and sub-degree accuracy was attained. Systematic errors affecting the solution accuracy are discussed, as are the results of an attempt to solve for sensor measurement angle biases in the state vector.

PRECEDING PAGE BLANK NOT FILMED

1. INTRODUCTION

The Kalman filter presented here was developed as part of a continuing effort in the Attitude Analysis Section (Code 554.1) at NASA/Goddard to investigate the potential of sequential filters for spacecraft ground attitude estimation. The filter was developed primarily to provide accurate real-time attitude determination for spinning spacecraft to complement the batch estimators that have been used up until now. Use of this filter or a successor is planned in support of upcoming spinning spacecraft missions such as SAMPEX/FAST.

Kalman filtering has the potential for obtaining attitude estimates of comparable, if not superior, accuracy to currently-used batch methods, since, like batch methods, it can use large numbers of measurements in its solution, while, unlike them, it also models dynamic noise. Moreover, it has the potential for doing this in real-time with minimal human operator involvement, unlike batch methods. The filter presented here was coded and run on a 286-class IBM PC clone, in part to demonstrate the potential of personal computers for computation-intensive attitude estimation.

A complete modeling of the dynamics of an asymmetrical, rigid spacecraft could probably be incorporated into a Kalman filter, using, for example, the equations given in Melvin (1989). Due to their complexity, however, it is not obvious that these equations could be propagated quickly enough for real-time attitude estimation using a PC. To retain a high degree of accuracy while ensuring real-time performance, the highly linear dynamics model used by Markley, et.al. (1988), which models the nutational motion of an axisymmetrical rigid body, has been used.

Measurement equations are developed which, given a sensor complement of a single Sun sensor and a single Earth sensor, permit the filter to solve for the nutating three-axis attitude of a spinning spacecraft. A discussion of systematic errors affecting the spin axis estimate is given last, and those errors which may be compensated for or solved for in the filter are noted.

2. DYNAMICS MODEL

Spinning spacecraft are usually designed to spin about a nominal spin axis, taken here as the body Z axis, $\mathbf{Z}_b$. The deployment process usually imparts a nutational motion to the spacecraft, however, which causes the nominal spin axis to move on a elliptical cone about the spacecraft angular momentum vector **L** at the inertial nutation rate w_1. If the principle axis of the spacecraft $\mathbf{Z}_p$ is offset from $\mathbf{Z}_b$, it is $\mathbf{Z}_p$ that nutates about **L**, while $\mathbf{Z}_b$ revolves on a circular cone about $\mathbf{Z}_p$ at the body nutation rate w_b in a motion called "coning" (Wertz, p.489). Since the angular measurements returned by the attitude sensors are referenced to $\mathbf{Z}_b$, its motion must be modeled for accurate attitude estimation. It should be noted that most spacecraft have nutation dampers to reduce inertial nutation, but this motion is present to some degree most of the time.

The attitude of the spacecraft, given as the attitude matrix A_{pi} which transforms a vector in an inertial frame into the spacecraft principle axis frame, may be represented as the product:

$$A_{pi}(t) = A_{pl}(t)\ A_{li}(t) \qquad (1)$$

where
$$A_{li}(t) = A_2(\pi/2-\delta)\ A_3(\alpha)$$
$$A_{pl}(t) = A_3(\psi)\ A_1(\theta)\ A_3(\Phi)$$

and where $A_j(\Gamma)$ represents a rotation Γ about the jth body axis (Markley, et.al., (1988)). Matrix A_{li}, which transforms a vector into an intermediate frame with the spacecraft angular momentum vector along its Z axis, is introduced to separate the motions of **L** and $\mathbf{Z}_p$. This is done since, for most spinning spacecraft, the spin rate is chosen so that the integrated magnitude of all disturbance torques acting on the spacecraft is negligible compared to the magnitude of the angular momentum vector **L**. In this case, the direction of **L** remains essentially constant, and A_{li} is therefore constant as well; the spin axis attitude of the spinning spacecraft is generally defined as the angular momentum direction. Note that if the angular momentum direction were to change rapidly, this motion could be modeled with a variation of parameters approach (Kraige and Junkins (1976)).

Angles Φ, θ, and ψ, which define the nutational motion of the spacecraft about **L**, are given by complicated elliptic

functions in time for the general case of a spacecraft with unequal transverse principle moments of inertia (those perpendicular to the spin axis) (Melvin (1989)). In the interest of filter run-time performance, the filter presented here models only the axisymmetrical case, in which the two transverse principle moments of inertia are equal.

With the spacecraft assumed to be an axisymmetrical rigid body experiencing negligible external torques, the attitude and dynamics of the spacecraft may be described by the following state vector equations (Markley, et.al. (1988)):

$$\mathbf{x} = [\ \alpha,\ \delta,\ \Phi,\ \theta,\ \psi\ ,\ w_1,\ w_p\ ]^T \qquad (2)$$

$$\dot{\mathbf{x}} = [\ 0,\ 0,\ w_1,\ 0,\ w_p,\ 0,\ 0\ ]^T \qquad (3)$$

where

$\alpha,\ \delta$ = the right ascension and declination of the angular momentum vector in geocentric inertial (GCI) coordinates;

Φ,θ,ψ = three 3-1-3 Euler angles specifying the attitude of the nutating spacecraft with respect to the angular momentum reference frame, where θ is the constant nutation angle and where Φ and ψ are (for small nutation angles) basically rotations about the spin axis; the sum $\Phi+\psi$ is approximately equal to the "phase angle";

w_1 = the inertial nutation rate at which $\mathbf{Z}_p$ nutates about the angular momentum vector $\mathbf{L}$;

w_p = the body nutation rate at which $\mathbf{Z}_b$ cones about $\mathbf{Z}_p$.

3. MEASUREMENT MODEL

This analysis assumes that all attitude measurements received by the spacecraft are represented as the angle between the nominal spacecraft spin axis, $\mathbf{Z}_b$, and a sensed reference vector, $\mathbf{V}$, known precisely in the inertial frame. The time of this angular measurement is also used. While this model is a simplification of measurements obtained by real sensors, it

captures the essential attitude information and permits the results to be compared easily with other vector-based approaches, such as that, for example, given by Schuster (1983).

For each angle/time pair received from a each sensor, three measurements are calculated as follows:

$$z_1 = \cos(\Omega) \tag{4}$$

$$z_2 = 0. \tag{5}$$

$$z_3 = 2\pi / (t_2 - t_1). \tag{6}$$

where

Ω = measured angle between $\mathbf{V}$ and $\mathbf{Z}_b$
t_2 = time of measurement
t_1 = time of previous measurement of $\mathbf{V}_i$ by same sensor

The first measurement corresponds to the measured angle itself, the second to the sine of a reference phase angle at the measurement time, and the third to the total spin rate.

These actual measurements received from the sensors are compared to three corresponding expected measurements calculated by the filter from the propagated state estimate as follows:

$$h_1 = \mathbf{V}_i \cdot \mathbf{Z}_{b,i} = \mathbf{V}_i^T [A_{il}(\alpha,\delta)] [A_{lp}(\Phi,\Theta,\Psi)] \mathbf{Z}_{b,p} \tag{7}$$

$$h_2 = \mathbf{V}_i \cdot \mathbf{T}_i = \mathbf{V}_i^T [A_{il}(\alpha,\delta)] [A_{lp}(\Phi,\Theta,\Psi)] \mathbf{T}_p \tag{8}$$

$$h_3 = w_l + w_b \tag{9}$$

where $\mathbf{T}_p = (\mathbf{B}_p \times \mathbf{Z}_{b,p}) / |\mathbf{B}_p \times \mathbf{Z}_{b,p}|$

and
A_{il} -- the angular momentum-to-inertial attitude matrix
A_{lp} -- the principle-to-angular momentum attitude matrix
$\mathbf{T}_p$ -- the measurement "trigger vector", principle frame
$\mathbf{B}_p$ -- Sensor boresight vector, principle frame
$\mathbf{Z}_{b,p}$ -- the body Z axis $\mathbf{Z}_b$ in the principle axes frame
$\mathbf{Z}_{b,i}$ -- the body Z axis $\mathbf{Z}_b$ in the inertial frame
Note: all the vectors above are of unit length.

The difference **h-z** between the expected and actual measurements is used to update the filter state and covariance. Note that the measurement equations are non-linear in the state parameters. Because of this, the notation and equations for the extended Kalman filter have been used here.

4. KALMAN FILTER ALGORITHM

In this study, the standard extended Kalman filter equations have been used, given as follows (Gelb, p.188):

State estimate and error covariance dynamic propagation:

$$\dot{\mathbf{x}}(t) = \mathbf{f}(\mathbf{x}(f),t) \tag{10}$$

$$\dot{P}(t) = F(\mathbf{x}(t),t)P(t) + P(t)F^{T}(\mathbf{x}(t),t) + Q(t) \tag{11}$$

State estimate and error covariance measurement update:

$$\mathbf{x}_k(+) = \mathbf{x}_k(-) + K_k\,[\mathbf{z}_k - \mathbf{h}_k(-)] \tag{12}$$

$$P_k(+) = [I-K_kH_k(-)]\,P_k(-)\,[I-K_kH_k(-)]^T + K_kR_kK_k^T \tag{13}$$

where

$$K_k = P_k(-)H_k^T(-)\,[\,H_k(-)P_k(-)H_k^T(-) + R_k]^{-1} \tag{14}$$

For a complete development of the theory and meaning of these equations, see the Gelb reference. The Joseph update in equation (13) was found to be necessary for numerical stability, while iterating the measurement update (Gelb, p.190) was found useful for converging large errors in the a priori estimate.

5. FILTER PERFORMANCE WITH SIMULATED DATA

A truth model was developed to provide realistic measurements to the filter for a range of attitudes and dynamics for testing purposes. The true spacecraft attitude and dynamics were given by:

$$\mathbf{x} = [\,\alpha,\ \delta,\ \Phi,\ \Theta,\ \psi\ ,\ w_1,\ w_p\,]^T \tag{15}$$

$$\dot{\mathbf{x}} = [\,0,\ 0,\ w_1,\ 0,\ w_p,\ 0,\ 0\,]^T + \mathbf{U} \tag{16}$$

basically the same model used in the filter, except with U, the dynamic noise, added (Markley, et.al., (1988)). While this truth model does not account for the effects of external torques and does not model the dynamics of non-axisymmetrical spacecraft, it does permit the testing of the filter without the interference of modeling error.

A battery of filter runs were performed to test the convergence of the filter from a variety of a priori state estimates. For these tests, only the data from a single Sun sensor and a single Earth sensor were used to update the state estimate. The covariance results of these tests showed that state parameters Φ, ψ, w_1, and w_p were in all cases highly correlated, to the largest degree in the tests where the nutation angle θ was small. Because of this high correlation, the filter was able to estimate the angles Φ and ψ to only within about 5° at best.

Because of measurements h_2 and h_3 on the phase angle and spin rate, respectively, the filter was however able to estimate the sums $\Phi+\psi$ (the phase angle) and w_1+w_p (the spin rate) quite accurately. Since most spinning spacecraft may be supported adequately without the need for knowing the phase angle, much less the component angles Φ and ψ, the above observability problem would probably not be an operational concern as long as the attitude would be solved for adequately. Indeed, despite the 5° error in Φ and ψ, the filter solves for the spin axis attitude in terms of α and δ to sub-degree accuracy in all the test cases that were run.

An explanation for the observability problem noted above follows. The phase angle $\Phi+\psi$ and spin rate w_1+w_p are estimated quickly and accurately by measurements h_2 and h_3, respectively. The only information to distinguish between Φ and ψ and between w_1 and w_p, however, comes from measurement h_1, the cosine of the angle between the body Z axis and the sensed reference vector. The measured angle will oscillate sinusoidally with amplitude θ and angular rate w_1 as the spacecraft principle Z axis rotates about the angular momentum vector at the inertial nutation rate. Also, the location of the angle on this sinusoidal curve permits only two possibilities for angle Φ. For larger nutation angles θ the filter can isolate both Φ and w_1 using the variation in h_1, allowing for a fairly accurate determination of Φ, ψ, w_1, and w_p when combined with measurements h_2 and h_3. For cases of small

nutation angles or large measurement noise on h_1, however, the sinusoidal variation in h_1 becomes difficult to distinguish and the uncertainty in Φ, ψ, w_1, and w_p becomes larger. In contrast to a 5° best-case uncertainty in Φ and ψ, the uncertainty may grow to 30° or more for the smallest nutation angles. Simulations have shown, however, that when the nutation angle becomes small enough to cause large errors in Φ and ψ, it is also so small that it does not significantly affect the spin axis determination either.

5.1 SAMPLE CONVERGENCE RESULTS

Figures 1 to 3 illustrate how the state estimate converges from three different large a priori state errors. The true state is compared to the Kalman filter estimate, and two error terms are calculated. The spin axis error is approximated by:

$$SAE = [\ d^2(\alpha) + d^2(\delta)\ ]^{.5} \tag{17}$$

while the error in a "reduced state" with components $\Phi+\psi$ and w_1+w_p, instead of Φ, ψ, w_1, w_p, is given by:

$$RSE = [\ d^2(\alpha) + d^2(\delta) + d^2(\Phi+\psi) + d^2(\theta) + d^2(w_1+w_p)\ ]^{.5} \tag{18}$$

In these equations, $d^2(\ )$ represents the square of the difference between the estimated and actual values of the parameter in parentheses.

The initial conditions for these runs are given in the Appendix. Figure 1 shows that the filter almost immediately solves for the spin axis to an uncertainty of only about 0.1° from an a priori state with a 20° error. A more realistic convergence scenario is illustrated in Fig. 2 for an a priori estimate with errors on the order of 70° for Φ and ψ, and on the order of 20° for their sum. In practice, these angles should be the most difficult state initialization parameters to calculate, so these large errors are appropriate. Figure 2 shows that the filter takes substantially longer to converge, but solves for the spin axis to the same 0.1° uncertainty level after about a minute.

Figure 3 illustrates convergence from an a priori state with errors on the order on 5 deg/sec for w_1 and w_p and 2 deg/sec for their sum. The filter has the most difficulty converging with

large nutation rate errors, because they generate large errors in Φ and ψ, as well, during convergence. This difficulty is reflected in Figure 3, which shows that the filter requires over five minutes to converge to a 0.1° spin axis attitude uncertainty. The large value of the error in the reduced state is caused by the filter converging to a negative value of the nutation angle θ; this result is perfectly acceptable, and serves to illustrate that angle Φ was driven 180° from its a priori value due to the high a priori rate errors. It should be noted that a priori rate errors as large as these should never have to be input into the filter, since w_1 and w_p can be calculated accurately beforehand, given the spin rate and moments of inertia of the spacecraft (Wertz, p.490).

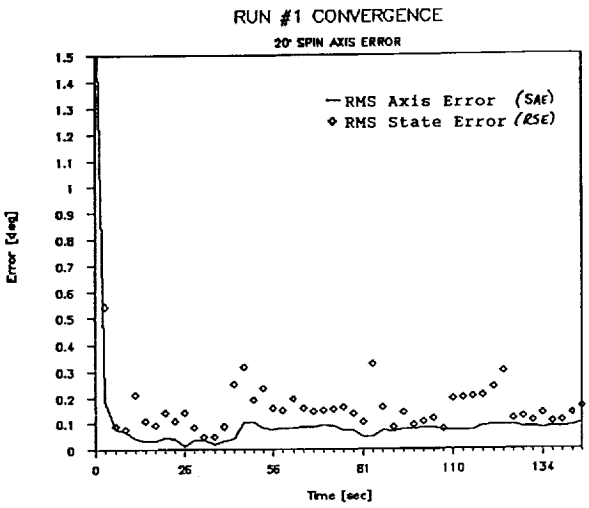

Figure 1.
Large A Priori Spin Axis Attitude Error

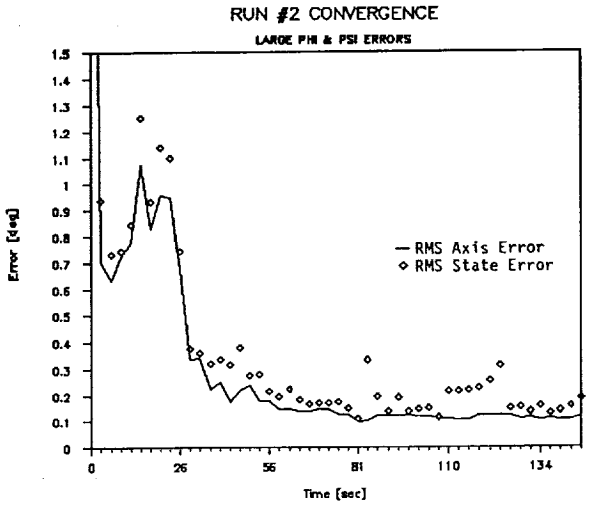

Figure 2.
Large A Priori ϕ and ψ Errors

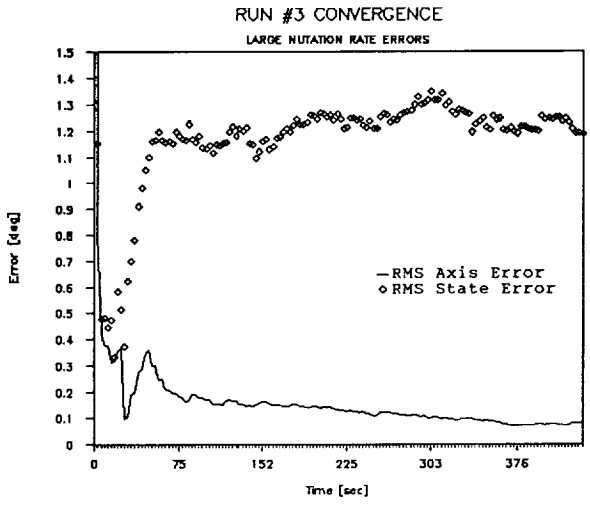

Figure 3.
Large A Priori Nutation Rate Errors

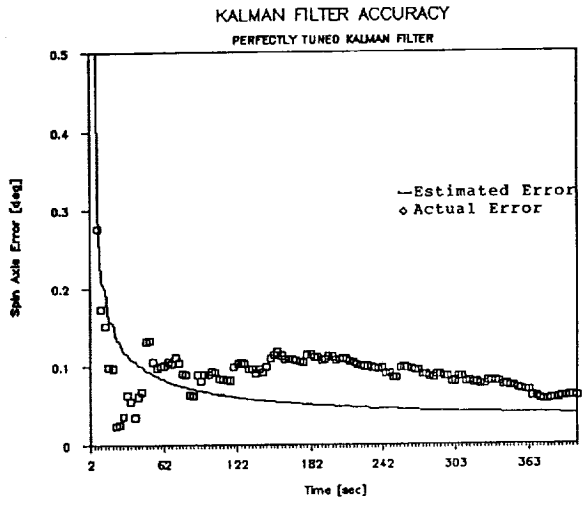

Figure 4.
Perfectly Tuned Kalman Filter

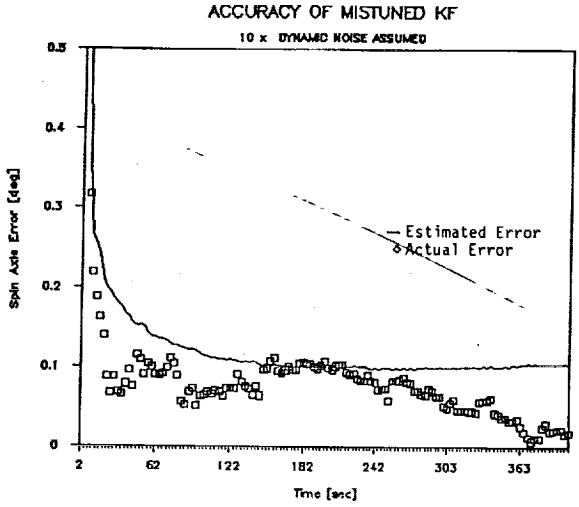

Figure 5.
Assumed Dynamic Noise 10x Too Large

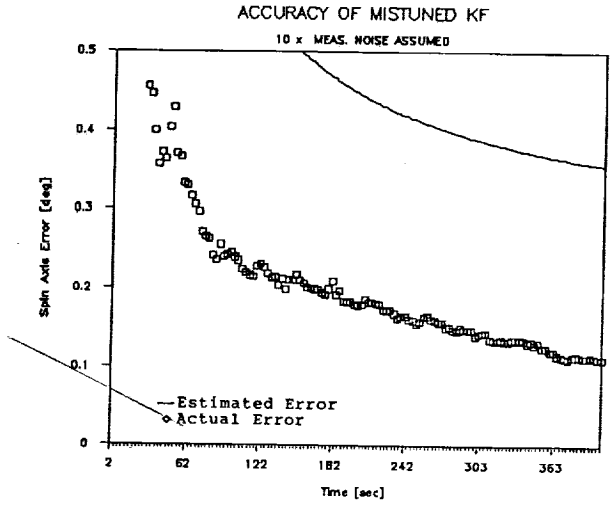

Figure 6.
Assumed Measurement Noise 10x Too Large

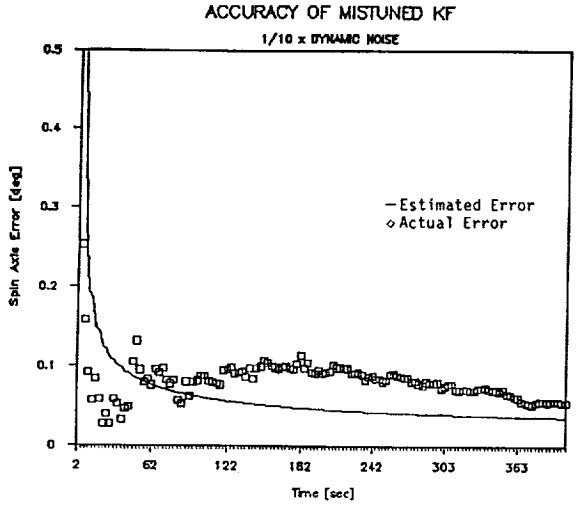

Figure 7.
Assumed Dynamic Noise 10x Too Small

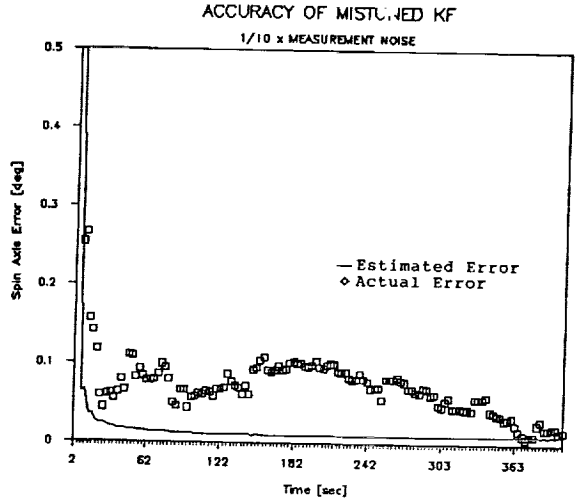

Figure 8.
Assumed Measurement Noise 10x Too Small

5.2 ACCURACY RESULTS

The user of a Kalman filter is required to make an estimate the magnitude of the dynamic and measurement noise affecting the system and the data being filtered. The magnitude of this noise is usually not known exactly, especially in the case of the dynamic noise, and may not even be known to within an order of magnitude. Since the magnitude estimate of these noise terms is always in error to some degree, it is interesting to see how such "mistuning" effects the filter results. The truth model enables the actual error in the state estimate to be compared against the

Kalman filter covariance, which indicates how well the filter believes it is estimating the state.

Figures 4 through 8 plot as a function of time both the actual spin axis error, approximated by equation (17) (the difference between the true values and the KF estimates), and the Kalman filter covariance corresponding to the same error. Figure 4 gives these results for a perfectly tuned filter, Figures 5 and 6 for assumed values for dynamic and measurement noise 10 times too high, respectively, and Figures 7 and 8 for those same respective noises assumed to be 10 times to low. While the actual and estimated errors do not agree exactly, even in the perfectly tuned case, an overriding tendency can be noted: the accuracy of the Kalman filter covariance seems to be much more sensitive to the assumed measurement noise magnitude than to the assumed dynamic noise magnitude. This is fortunate, since the properties of the dynamic noise are usually known less well than those of the measurement noise.

The parameters used the accuracy runs above are given in the Appendix. In additional runs not shown here, for which the dynamic noise and measurement noise were set to zero in both the truth model and the Kalman filter, the actual and estimated errors were both extremely low, as would be expected, since the filter and truth model both use the same dynamics model.

5.3 FILTER SPEED

Besides achieving sub-degree accuracy, the Kalman filter for the runs above was able to propagate and update in real time. This was achieved by choosing an appropriate value for the propagation step size; this step size could be set quite large because of the linearity of the dynamics. Since the test cases above were run assuming a spacecraft spin rate of about 10 rpm, and since two measurements were assumed to be received each spin period (a Sun angle and an Earth angle), the filter had to process a measurement update every 3 seconds on the average to operate in real time. The runs were executed on a 12 MHz 286-class IBM PC clone. Use of a faster 386-class machine would permit smaller dynamic propagation steps to be taken, or, alternatively, a larger number of measurements to be processed per spin period.

6. PERFORMANCE WITH ACTUAL SPACECRAFT DATA

Attitude sensor data were obtained from the DE-A spacecraft in order to test the potential of the Kalman filter for actual spacecraft ground attitude determination. The author was unable to obtain data for a period with significant nutational motion, however, so the following results only validate the filter's performance for the nutationally-damped case.

Data from a single Earth sensor and a single Sun sensor were entered into the Kalman filter as input. Nadir angles had to be calculated beforehand from the original DE-A Earth sensor data, and precalculated biases were subtracted from the Sun angles before they were input, as well.

TABLE 1 -- KF INPUT FOR DE-A DATA RUN

$\mathbf{x}_o$ = [1.1968,-.17216, 0., 0.,-1.3209, -1.9568, .89226]^T
Dynamic noise =
[.001, .001, .005, .002, .005, .002, .002]^T
Measurement noise = [.0002, .01, .0002]^T
$\mathbf{z}_b$, principle frame = [0., 0., 1.]^T
Uncert. in $\mathbf{x}_o$ = [.03, .03, 1.0, .005, 1.0, .001, .001]^T

The filter input parameters for the run are given in Table 1. The estimated filter spin axis right ascension and declination are plotted in Figures 9 and 10, with the batch solution plotted as the straight line on the same plots. As Table 2 shows, the difference between the Kalman filter and batch spin axis directions is within the 0.21 degree uncertainty given by both the Kalman filter and batch methods. The fact that the Kalman filter and batch covariances agree so closely suggests that level of dynamic noise, which the batch method does not model, is of negligible significance in this data as compared with the level of measurement noise.

TABLE 2 -- COMPARISON OF KF & BATCH SOLUTIONS

	Batch	KF	Difference
Spin Axis RA [deg]	68.2610	68.35	+0.089
Spin Axis Dec [deg]	-9.4650	-9.54	-0.075
Spin Axis Att [deg]			0.116
Att. Uncert. [deg]	0.2178	0.21	

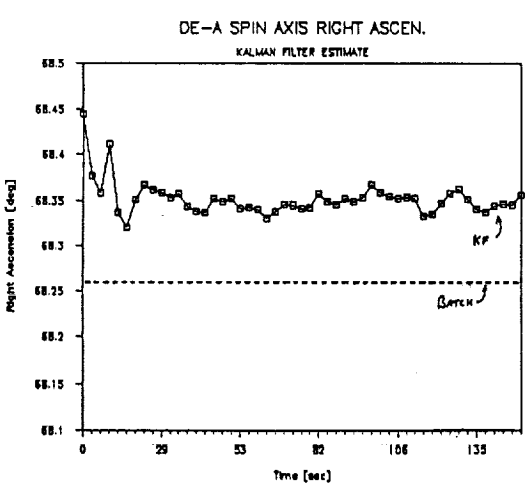

Figure 9.

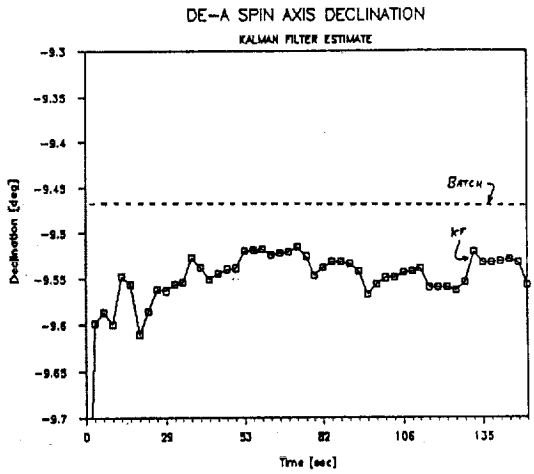

Figure 10.

7. UNMODELED ERROR SOURCES

7.1 SPACECRAFT ASYMMETRY EFFECTS

The Kalman filter described above successfully solves for the nutating 3-axis attitude of an axisymmetrical spinning spacecraft. No spacecraft is truly axisymmetrical, however, since the two principle moments of inertia perpendicular to the spin axis are always unequal to some degree. The Kalman filter estimate will therefore suffer from modeling error when real data from a nutating spacecraft is filtered. The Kalman filter should in this case try to model the elliptical path of $\mathbf{z}_p$ about $\mathbf{L}$ for the real spacecraft with a circular path. The modeling error would depend on the extent of the spacecraft asymmetry, and would cause both an increase in the uncertainty of the spin axis attitude uncertainty and a shift in the solved-for spin axis direction (Wertz, p.541). This error source could be removed by correctly modeling the dynamics of an asymmetric spacecraft, perhaps with a state based on the dynamics model of Melvin (1989).

7.2 SENSOR BIASES AND MISALIGNMENTS

If not compensated for, sensor biases and misalignments can cause large shifts in the solved-for spin axis direction. A bias or misalignment that systematically changes the measured angle between the spacecraft body Z axis and the reference vector may cause a shift in the estimated spin axis direction: using the analogy of the cone method attitude solution (Wertz, p.363) for an Earth and Sun sensor, the spin axis direction, lying along the intersection of the Sun and Earth cones, changes as the Sun and Earth angles change from their true to their biased values. As discussed below, attempts to solve for Sun and Earth angle biases by adding them to the state vector were not successful. The filter given above could easily compensate for precalculated angle biases, however, by subtracting these biases from the measured angles before using them in the update equations.

The relative misalignment of sensors in the plane perpendicular to the body Z axis would change the timing of the angular measurements, affecting the accuracy of the estimated Φ and ψ angles, the w_l and w_p nutation rates, and, to a much lesser extent, the spin axis direction, as well.

7.3 Z_p OFFSET FROM Z_b

If the principle Z axis, $\mathbf{Z}_p$, of the spacecraft is offset from the body Z axis, $\mathbf{Z}_b$, due to non-zero products of inertia I_{xz} and I_{yz}, then $\mathbf{Z}_b$ will "cone" about $\mathbf{Z}_p$ at the body nutation rate (see Wertz, p.490). This coning motion will add a sinusoidally-varying error to measurements taken at a rate other than the spin rate (e.g., from a magnetometer), but will simply add a constant bias to measurements taken at the spin rate (e.g., from a Sun or Earth sensor) since the direction of $\mathbf{Z}_b$ relative to $\mathbf{Z}_p$ and the sensed reference vector $\mathbf{V}$ is the same for subsequent measurements.

This bias may result in a systematic error in the estimated spin axis direction for filters that assume $\mathbf{Z}_b$ and $\mathbf{Z}_p$ are collinear. The effects of the $\mathbf{Z}_b/\mathbf{Z}_p$ offset may be removed in this Kalman filter, however, simply by entering the value of $\mathbf{Z}_b$ in the spacecraft principle reference frame into the measurement equations (7) and (8). Vector $\mathbf{Z}_b$ in the principle frame may be calculated from the mass moment of inertia matrix.

8. SENSOR MISALIGNMENT ESTIMATION PROBLEM

An attempt was made to solve for the angular biases noted above in the Kalman filter, in hopes of removing this major source of spin axis attitude error. A Sun angle bias and an Earth angle bias were added to the state and dynamics model, and the measurement equations were modified to account for the bias terms. The truth model then produced simulated angular measurements shifted by specified Sun and Earth biases, and the Kalman filter was applied to the data to solve for the specified biases along with the attitude.

The filter was unable to solve for the applied biases, however, due to high correlations between these biases and the attitude parameters. In particular, the filter was unable to differentiate between the angular biases and errors in the spin axis direction. A covariance analysis was performed using the Attitude Determination Error Analysis System (ADEAS) (Nicholson, et.al. (1988)) to determine to what accuracy the biases could be expected to be solved for. The ADEAS results suggested that for normal noise levels the biases could not be determined in the Kalman filter to a useful level of accuracy.

9. CONCLUSION

In this paper, a new Kalman filter has been presented that solves for the nutating 3-axis attitude of a spinning spacecraft in real-time on a 286-class IBM PC clone to an accuracy comparable to or better than the batch methods currently used. The filter has been tested both with simulated data and with real data from the DE-A spacecraft. Although a modified version of the filter was unsuccessful in solving for biases on the measured angles, the filter could compensate for these errors if biases calculated in some other way were to be input into the filter. Similarly, the filter can remove errors due a $\mathbf{Z}_p/\mathbf{Z}_b$ offset by using the easily-calculated $\mathbf{Z}_{b,p}$ vector as input.

Attitude errors due to unequal spacecraft transverse moments of inertia cannot be compensated for in this filter. Further work on removing this error source by properly modeling the general motion of an asymmetrical rigid body would be valuable.

REFERENCES

Dynamics Explorer -A and -B Attitude System Functional Specifications and Requirements, OAO Corporation, Beltsville, Maryland, under contract No. NASA-25534, December, 1979.

Fang, B.T., "Mathematical Specifications for an Attitude/Orbit Error Analysis System", Planetary Sciences Dept., Report No. 009-74 under Contract No. NAS 5-20098, October, 1974.

Gelb, A., ed., Applied Optimal Estimation, The MIT Press, 1974.

Kraige, L.G., and J.L. Junkins, "Perturbation Formulations for Satellite Attitude Dynamics", Celestial Mechanics, Vol 13. (1976), pp. 39-64.

Markley, F.L., E. Seidewitz, and M. Nicholson, "A General Model for Attitude Determination Error Analysis", Proceedings of the Flight Mechanics/Estimation Theory Symposium, May 1988.

Melvin, P.J., "A New Method for Generation of Torque Free Motion of a Satellite", AIAA Paper No. 89-0546.

Nicholson, M., F.L. Markley, and E. Seidewitz, Attitude Determination Error Analysis (ADEAS) Mathematical Specifications Document, CSC/TM-88/6001, Computer Sciences Corporation, October 1988.

Schuster, M.D., "Efficient Algorithms for Spin Axis Attitude Estimation", The Journal of the Astronautical Sciences, Vol. 31, No. 2, pp. 237-249, April-June, 1983.

Wertz, J.R., ed., Spacecraft Attitude Determination and Control, D. Reidel Publishing Company, Boston, 1978.

APPENDIX

CONVERGENCE TEST PARAMETERS

Truth Model Input: ($\mathbf{x} = [\alpha, \delta, \Phi, \theta, \psi, w_1, w_p]^T$)

$\mathbf{x}_o$ = [1.222, -.349, 1., .01, 1., 1.925, -.8777]^T

Dynamic noise = [.00001, .00001, .005, .0002, .005, .003, .003]^T

Measurement. noise = [.002, .002, .002]^T

$\mathbf{z}_b$, principle frame = [0., 0., 1.]^T

Base Parameters for KF Runs:

$\mathbf{x}_o$ = [1.172, -.399, .83, .0, .915, 1.915, -.8727]^T

Dynamic noise = [.000015, .000015, .0075, .0003, .0075, .0045, .0045]^T

Measurement. noise = [.003, .003, .003]^T

$\mathbf{z}_b$, principle frame = [0., 0., 1.]^T

Uncert. in $\mathbf{x}_o$ = [.05, .05, .17, .02, .17, .01, .01]^T

Run #1 -- Large A Priori Spin Axis Attitude Error

$\mathbf{x}_o$ = [1.469, -.596, .83, .0, .915, 1.915, -.8727]^T

Uncert. in $\mathbf{x}_o$ = [.25, .25, .17, .02, .17, .01, .01]^T

Run #2 -- Large A Priori Φ and ψ Errors

$\mathbf{x}_o$ = [1.172, -.399, -.2, 0., 2.6, 1.915, -.8727]^T

Uncert. in $\mathbf{x}_o$ = [.05, .05, 1.5, .02, 1.5, .01, .01]^T

Run #3 -- Large A Priori Nutation Rate Errors

$\mathbf{x}_o$ = [1.172, -.399, .83, .0, .915, 1.82, -.8077]^T

Uncert. in $\mathbf{x}_o$ = [.05, .05, .17, .02, .17, .2, .2]^T

(Units: angles in radians, rates in radians/second)

ACCURACY TEST PARAMETERS

Truth Model Input: ($\mathbf{x} = [\alpha, \delta, \Phi, \theta, \psi, w_l, w_p]^T$)

$\mathbf{x}_o$ = [1.222, -.349, 1., .01, 1., 1.925, -.8777]^T

Dynamic noise = **D** =
[.00001, .00001, .005, .0002, .005, .003, .003]^T

Measurement noise = **M** = [.002, .002, .002]^T

$\mathbf{Z}_b$, principle frame = [0., 0., 1.]^T

Base Parameters for KF Runs:

$\mathbf{X}_o$ = [1.172, -.399, .83, .0, .915, 1.915, -.8727]^T

$\mathbf{Z}_b$, principle frame = [0., 0., 1.]^T

Uncert. in $\mathbf{X}_o$ = [.05, .05, .17, .02, .17, .01, .01]^T

Run #1 -- Perfectly tuned KF
Dynamic noise = **D**
Measurement noise = **M**

Run #2 -- Assumed Measurement Noise 10x Too Large
Dynamic noise = **D**
Measurement noise = 10. x **M**

Run #3 -- Assumed Dynamic Noise 10x Too Large
Dynamic noise = 10. x **D**
Measurement noise = **M**

Run #4 -- Assumed Measurement Noise 10x Too Small
Dynamic noise = **D**
Measurement noise = .10 x **M**

Run #5 -- Assumed Dynamic Noise 10x Too Small
Dynamic noise = .10 x **D**
Measurement noise = **M**

(Units: angles in radians, rates in radians/second)